fibers

MDPI

Article

Physico-Mechanical, Thermal and Biodegradation Performance of Random Flax/Polylactic Acid and Unidirectional Flax/Polylactic Acid Biocomposites

Mahmudul Akonda [1], S. Alimuzzaman [2], D. U. Shah [3] and A.N.M. Masudur Rahman [2,*]

[1] Department of Textile Engineering, Southeast University, Dhaka 1208, Bangladesh; mhakonda@yahoo.com
[2] Department of Fabric Engineering, Bangladesh University of Textiles, Dhaka 1208, Bangladesh; sazaman_2006@yahoo.com
[3] Centre for Natural Material Innovation, Department of Architecture, University of Cambridge, Cambridge CB2 1PX, UK; dus20@cam.ac.uk
* Correspondence: masudfabric@yahoo.com; Tel.: +880-15-5334-2607

Received: 11 August 2018; Accepted: 30 November 2018; Published: 10 December 2018

Abstract: Fully biodegradable flax/polylactic acid (PLA) thermoplastic composites were fabricated by using random (nonwoven mat) and aligned (unidirectional yarn) flax fiber as reinforcements (39% flax by volume) and Polylactic acid (PLA) as matrix. Results revealed that the aligned flax fibers have a greater reinforcing effect due to the uniform distribution of load axially along the fiber length in the composite. The aligned flax/PLA and random flax/PLA showed the tensile strength of (83.0 ± 5.0) and (151.0 ± 7.0) MPa respectively and flexural strength of (130.0 ± 5.0) and (215.0 ± 7.2) MPa respectively. Young's modulus of (9.3 ± 1.5) and (18.5 ± 2.0) GPa and flexural modulus of (9.9 ± 1.0) and (18.8 ± 1.0) GPa was attained for the random and unidirectional fiber composites, respectively. It was also found that both composite constituents, fiber and matrix, were degradable if buried in compost soil (ready soil after composting process), which is a distinctive advantage of the new composite structures. Remarkably, the biodegradation property of aligned flax fiber composites was significantly lower than random mat composites, possibly due to the less water swelling behavior of the aligned fiber composites. After 120 days burial test, the aligned flax/PLA composite displayed the reduction of 19% mass, residual flexural strength and modulus decreased by 57 and 50% respectively, while the random mat composites exhibited the loss of 27% mass, residual flexural strength and modulus declined by 80% at the same period.

Keywords: PLA; flax; thermoplastic composites; mechanical properties; biodegradability; durability

1. Introduction

Composite materials based on natural and renewable resources have received amazing interest in recent years due to a drive towards sustainable manufacturing and materials end-of-life management. It is well known that typical high-performance composite components, such as carbon and glass fibers and petrochemical-based matrices, require high energy for production, release considerable CO_2 into the atmosphere, are not biodegradable and not considered to be environmentally-friendly [1–3]. Also, the extreme consumption of petroleum-based plastics, which prompt massive volumes of non-decomposable wastes origins a thoughtful exhaustion of landfill dimensions. The wakefulness of climbed waste complications on the environment has stimulated a new concentration in the area of materials science. Because of the growing environmental awareness in the world, it is a critical issue for scientists to study diverse substitutions to switch non-biodegradable materials, particularly for petroleum-based products [4–7]. Consequently, various types of fully biodegradable resources are being developed recently, as replacements for non-renewable plastics. For a sustainable future,

environmentally friendly composite components (EFCs) with constituents that will be biodegradable at the end of usable life are of interest [8–10].

Biocomposites are the combination of biofibers with polymer matrices from both of non-renewable and renewable resources. Different types of biofibers such as jute [11], sisal [12], hemp [13], kenaf [14] and flax [15] have been investigated for reinforcing both thermoplastic and thermoset matrices. Biofibers are one of the major components of biocomposites and the fibrous material derived from plant sources. Biofiber composites are emerging as a sustainable alternate to glass fiber composites, mainly in packaging, automotive, building and consumer product industries and becoming one of the fastest rising additives for EFCs [16]. Among the commodity of biofibers, flax fibers show some unique mechanical properties. Other advantages such as production cost with low investment cost make it an interesting product for low-wage countries. Thermal recycling is also possible where glass causes problems in combustion furnaces. Flax fiber possesses low specific weight and higher stiffness than glass (Table 1). It also provides better thermal and acoustic insulation properties, especially as an automotive interior or construction material part [17,18].

Table 1. Comparison of glass fiber with some natural fiber properties [19,20].

Fiber Type	Density (g/m^3)	Tensile Strength (MPa)	Tensile Modulus (GPa)	Elongation at Break (%)	Moisture Absorption (%)
Glass	2.55	2000–3500	70–73	2.5–3	-
Flax	1.4–1.54	800–2000	60–85	1.2–4	7
Hemp	1.48	368–900	70	1.6	8
Jute	1.44–1.46	400–775	10–30	1.5–1.8	12
Sisal	1.33–1.5	350–700	22–38	2–7	11
Coir	1.25	220	6	15–25	10
Cotton	1.5–1.6	200–800	5.5–12.6	6–12	8–25

Although natural fiber reinforced thermoplastic composites are becoming more popular, particularly in the automotive industry but the options for the use of biodegradable thermoplastics are limited [21,22]. To obtain 'fully' biodegradable EFCs, the petrochemical-based matrix can be replaced by a vegetable-derived polymer, such as PLA. Among numerous ecofriendly polymers, PLA attracts particular attention for the improvement of engineering polymers [23,24]. PLA belongs to synthetic aliphatic polyesters (without branching between chains and strong entanglement). It is generally resulting from α-hydroxy acids, which are manufactured by means of monomer feedstock. PLA is produced through the condensation polymerization of a basic building block lactic acid (LA), which is generally made by microbial fermentation of carbohydrates (mainly hexose) in corn (glucose), cheese whey (lactose) and sugar cane (sucrose). Since PLA is compostable and derived from renewable, sustainable sources, it is regarded as a favorable material to improve collective solid waste disposal problems. However, contemporary applications of natural fiber/PLA thermoplastic materials are limited due to the mechanical properties of the composite [3,20,22,25,26].

To maximize the stiffness and strength of laminated composites, particularly for load-bearing applications, unidirectional reinforcements are the most preferable structures [27]. Usually, long natural fibers provide better mechanical properties to composite structures compared to short fiber reinforcements. However, the mechanical properties of composites also depend on other architectural parameters like fiber orientation, distribution, volume fraction and manufacturing effects (defects). As an example, flax mat/PP film sandwich structure shows poor mechanical properties compared to flax/PP commingled yarn composites due to poor fiber wettability. Similarly, due to damage of the fibers caused by needle punching during mat production process, needle-punched nonwoven mat of flax/PLA film structure provides reduced mechanical properties compared to flax yarn/PLA film structure [28]. Such parameters can also influence the water absorption and biodegradation properties of the composites.

The present research was focused on developing two different types of preforms such as random and aligned preforms produced from long flax fibers to manufacture flax/PLA composite. A novel air-laid technology was used to obtain fully-random flax reinforcements by avoiding needle-punching or film-stacking processes to maximize the reinforcing effect of fiber in nonwoven mat composites. In addition, a new commingled yarn structure from flax/PLA fiber blends was produced to fabricate composites. Thereafter, mechanical, water absorption and biodegradability performance of the biocomposite materials were evaluated.

2. Materials and Methods

2.1. Materials

Commercial grade flax (untreated) and short staple PLA fibers were sourced from Procotex and DS fibers, Belgium respectively. Some specifications of the used fibers and produced materials are presented in Table 2.

Table 2. Physical properties of flax, PLA fibers and their intermediate products.

Properties	Flax Fiber	PLA Fiber	Flax/PLA Nonwoven Mat	Flax/PLA Yarn
Fiber diameter (μm)	22.0 ± 1.0	28.0 ± 0.5	-	-
Linear density	6.6 ± 0.5 dtex	3.3 ± 0.5 dtex		250.0 ± 10.0 tex
Areal density	-	-	1000.0 ± 50.0 g/m^2	-
Mean fiber length (mm)	70.0 ± 17.0	70.0 ± 3.0	-	-
Tenacity (MPa)	750.0 ± 15.0	104.0 ± 5.0	-	-
Breaking elongation (%)	1.8 ± 0.5	2.9 ± 1.0	0.8 ± 1.0	3.5 ± 1.0
Melting temperature (°C)	-	171.0	-	-
Density (g/cm^3)	1.54	1.24	-	-

2.2. Evaluation of Fiber Property and Preform

Areal density (g/m^2) and the thickness of the preforms were tested. The areal density was determined according to ISO 9073-1: 1989 standard. The thickness was measured according to ISO 9073-2: 1997 standard by using Shirley thickness gauge under a pressure foot of 8 cm diameter and pressure of 250 gm.

To calculate the linear density of the fibers ISO 1973: 1996 standard was followed. According to the standard 10 fiber tufts having a mass of several milligrams were taken from the sample and the fibers of each tuft were brought into parallel arrangement. The middle part of each combed tuft was 50 mm in length. Five fibers were taken out from each of ten bundles in turn, so as to form a bundle of 50 fibers and 10 of these bundles were made. These bundles were weighted individually using the balance. The mean linear density of fiber in each bundle was calculated by Equation (1).

$$\rho_{l,b} = \frac{m_b}{n_f \times l_f} \times 10^4 \quad (1)$$

where, $\rho_{l,b}$ is the mean linear density of the fiber in each bundle in decitex (dtex); m_b is the mass of fiber bundle in mg; n_f is the number of fibers in the bundle; l_f is the length of the individual fibers in the bundle in mm.

The areal density was measured by the following equation:

$$M = \frac{m}{A} \times 10^6 \quad (2)$$

where, M is the areal density in g/m^2; m is the mass per sample area in gm; A is the area of the sample in mm^2.

2.3. Production of Flax/PLA Preforms

2.3.1. Aligned Flax Fiber Preforms

Flax fibers (sliver form) were commingled with staple PLA fibers at a ratio of 50:47 (wt.%) to produce a low twisted yarn structure. Conventional spinning process was used to produce flax/PLA yarn. The provided sliver form of flax and staple PLA fiber was passed through the carding and drawing process, rove is obtained by doubling of several number of slivers and finally yarn is produced by inserting 40 turn per meter (considered as low twist) in spinning frame. Additional 3% PLA were used as wrappers with a wrapping attachment in spinning frame to achieve 50% mass fraction of the PLA fibers in final yarns. The wrapper PLA was used as filament (150 dtex) form which was also collected from DS fibers, Belgium.

2.3.2. Randomly Aligned Flax Fiber Preforms

From the literature survey, it is found that most nonwoven preforms are made from stitch bonded mats. The stitch bonded nonwovens are based on needle punching, which can cause fiber damage [29]. The thermal bonding route used in this research work does not suffer from this drawback. The matrix material is also used as binding material here. The web is consolidated by using a hot pressing instrument.

Nonwoven webs (250 g/m^2) were prepared from flax/PLA blends using a mass ratio of 50:50 (wt.%) by means of an air laying process [30]. An air laying web forming machine generally consists of feeding, carding, stripping, transporting and condensing units which ensures the isotropic fiber orientation distribution, leading to isotropic composites. The mechanical properties of the composites are similar in all direction due to the isotropic fiber distribution [31]. Four layers of webs were piled-up together and the PLA fibers were partly melted to make a thicker 'batt' (mat) with an areal density of (1000 $\pm$ 50) g/m^2 to be used in the hot-press molding process. To ensure uniform blends, flax and PLA fibers were pre-opened manually prior to feeding into the nonwoven process. Nonwoven preform manufacturing technique is shown in Figure 1.

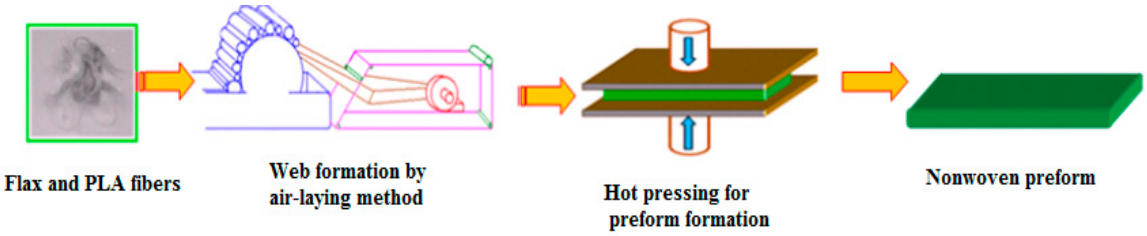

Figure 1. Schematic diagram of random flax preform fabrication process route.

2.3.3. Aligned Flax Fiber Composites

To obtain aligned fiber architecture in the composites, commingled yarns of flax/PLA were wound onto a steel frame (60 mm $\times$ 90 mm) unidirectionally. Six layers of yarn were subsequently compressed and consolidated using a hot compression molding process. The temperature was maintained 185 °C by keeping the pressure of 2 MPa for 5 min to produce 2.1 mm thick panels. The aligned (unidirectional) flax composites were termed as UD flax/PLA composites.

2.3.4. Randomly Aligned Flax Fiber Composites

To achieve random fiber architecture in the composites, two layers of nonwoven mats were used to produce 2.3 mm thick laminates. The molding parameters such as temperature and time were kept same as used for aligned laminates but higher pressure (4 MPa) was applied to compact the bulky mats and the produced composites were designated as NM flax/PLA composites.

2.4. Characterization of Composites

2.4.1. Mechanical Testing

The tensile properties of composite panels were measured in accordance with ISO 527-4:1997. The tests were conducted on a universal Instron testing machine, model 5569 with a 10 KN load cell at an extension rate of 2.0 mm/min. The Young's modulus was determined by considering a linear regression in the strain range of 0.0–0.2% [32]. Unidirectional composite samples were tested in the fiber direction. The flexural (3-point bending) tests were carried out according to ISO 14125:1998 by using another universal Instron testing machine, model 4411 with 5 KN load cell at a constant crosshead speed of 2.0 mm/min. For these tests the specimen size was maintained (60 mm × 25 mm × 2.1 mm) for UD flax/PLA and (60 mm × 25 mm × 2.3 mm) for NM flax/PLA composites. All tests were performed at 23 ± 2 °C temperature and RH 50 ± 5%. Five samples of each type were tested and the final values were taken as the average value of five measurements.

2.4.2. Density, Fiber Volume Fraction and Void Content Measurement

In order to calculate the constituents of the composite, it is necessary to separate the reinforcement and the matrix. For this purpose, the resin digestion method ISO 14127: 2008 was used. In this method, Dichloromethane (DCM) was used to digest the PLA matrix [33]. The desiccated mass of the specimen was determined before and after the matrix digestion. The composite specimens were soaked in a bath at room temperature to digest the matrix. Sintered glass crucibles, oven, desiccators, DCM, conical flax and weighing balance were used in this experiment. The density of each specimen was calculated from the mass and volume. For these experiments, the average values were calculated from five measurements and considered as final value.

The fiber content, void content and flax volume fraction were calculated using the following Equations (3)–(7):

$$W_f\ (\%) = \frac{m_3 - m_1}{m_2 - m_1} \times 100 \tag{3}$$

where, W_f is the fiber content as a percentage of the initial mass; m_1 is the sintered glass crucible (gm); m_2 is the initial mass of the specimen and glass crucible (gm); m_3 is the final total mass (gm) of the crucible and residue after digestion.

$$W_r = 100 - W_f \tag{4}$$

where, W_r is the PLA content as a percentage of the initial mass; W_f is the fiber content as a percentage of the initial mass.

$$V_f = W_f \times \frac{\rho_c}{\rho_f} \tag{5}$$

where, V_f is the fiber content as a percentage of the initial volume, W_f is the fiber content as a percentage of the initial mass, ρ_c is the density of the test specimen (g/m^3), ρ_f is the density of flax (g/m^3).

$$V_r = \left(100 - W_f\right) \times \frac{\rho_c}{\rho_r} \tag{6}$$

where, V_r is the PLA content as a percentage of the initial volume; W_f is the flax content as a percentage of the initial mass; ρ_c is the density of the test specimen (g/m^3); ρ_r is the density of PLA (g/m^3).

$$V_0 = 100 - \left[W_f \times \frac{\rho_c}{\rho_f} + \left(100 - W_f\right) \times \frac{\rho_c}{\rho_r}\right] \tag{7}$$

where, V_0 is the void content as a percentage of the initial volume, W_f is the fiber content as a percentage of the initial mass, ρ_c is the density of the test specimen (g/m^3), ρ_f is the density of flax fiber (g/m^3), ρ_r is the density of PLA (g/m^3).

2.5. Differential Scanning Calorimetry (DSC)

The DSC technique determines the quantity of heat either absorbed or released when a substance undergoes a physical or chemical change. Several parameters can be estimated by performing a DSC scan. These parameters include the glass transition temperature (T_g), melting temperature (T_m), melting enthalpy (ΔH_m) and crystalline level. The DSC measurements were carried out by TA Instrument DSC Q100. The heating and cooling rate were 10 °C/min. The samples were first scanned from −20 to 220 °C, followed by cooling to −20 °C and then reheating up to 220 °C in a second scan. T_m was determined from the maximum region of the endothermic melting peak and T_g was an inflection temperature from the baseline of the first heating cycle. The degree of crystallinity (X_c) was calculated by Equation 8 using data from the DSC curve of the first heating cycle.

$$X_c(\%) = 100 \times \frac{\Delta H_m}{\Delta H_f} \tag{8}$$

where ΔH_m is the heat of fusion of the neat PLA and its composites, ΔH_f is the heat of fusion for 100% crystalline PLA (93.7 J/g).

2.6. Water Absorption Test

Water absorption determines the water swelling behavior of the composites. Water absorption test of the composite samples was carried out according to ISO 62:2008 (method 1). The samples (60 mm × 60 mm × 2.1 mm for UD and 60 mm × 60 mm × 2.3 mm for NM panel) were immersed in a beaker containing 300 mL distilled water for 60 days at room temperature. Before immersion, the samples were dried in a vacuum oven at 50 ± 2 °C temperature for 24 h, cooled in a desiccator and then immediately weighted (m_1). During the test, samples were withdrawn from the water at 20 days intervals, gently blotted with tissue paper to remove excess water from the surface, immediately weighed (m_2) and again dipped into the water. Each m_1 and m_2 value was an average value of three measurements. The gained mass percentage C (%) of the specimens due to water absorption was calculated using Equation (9).

$$C\ (\%) = 100 \times \frac{m_2 - m_1}{m_1} \tag{9}$$

2.7. Biodegradability Test

Biodegradability is one of the most important properties of the biocomposites. Soil burial test is the most widely used method to evaluate the biodegradability of the composite material. Different types of soil and compost have been used for biodegradation test. Kim et al. [34] showed that the biodegradability of the composite materials in compost soil is superior to that in a natural soil environment. Burial test was carried out in a flower pot containing Miracle Gro. moisture controlled compost soil [34,35]. The samples (60 mm × 25 mm × 2.1 mm for UD flax and 60 mm × 25 mm × 2.3 mm for NM flax panel) were buried randomly in compost soil for 4 months at a depth of 12–15 cm from the soil surface to ensure aerobic degradation [36]. The pots were covered with plastic film to avoid water evaporation from the compost surface. The P^H was maintained at 7 using a moisture meter and moisture content was preserved 40–50% by sprinkling water at an interval of 2 days. Biodegradation was estimated by monitoring changes in mass and mechanical properties (flexural bending) as a function of burial time. The samples were washed with water for the removal of debris on the specimen and finally dried at 60 ± 2 °C temperature for 24 h in air-dried woven before undergoing mass loss and mechanical properties test. Five replicates were evaluated for each type of samples for each test.

The percentage mass loss of treated samples was measured using an electronic balance and determined by Equation (10).

$$\text{Mass Loss } (\%) = \frac{M_i - M_d}{M_i} \times 100 \quad (10)$$

where, M_i is the initial mass and M_d is the mass after the designated burial day. The percentage mass loss was taken from the average of five samples.

Flexural tests for buried samples were conducted according to ISO14125:1998. The deterioration of flexural properties was assessed and the residual flexural property was evaluated using Equation (11).

$$\text{Residual flexural property } (\%) = \frac{P}{P_0} \times 100 \quad (11)$$

where P is the flexural strength or flexural modulus measured after the designated burial day and P_0 is the initial property before burial test.

2.8. Scanning Electron Microscopy (SEM)

A SEM (Philips XL30) was used to study the morphology of the surface degradation of neat PLA, composites and fracture surface of the test specimens. Flax fiber diameter was also measured to obtain the fiber linear density. The surface of the specimens was coated with carbon using an Edward coating system (E306A, USA).

3. Results and Discussion

Figure 2a indicates the produced nonwoven mats of flax/PLA fibers. Figure 2b shows flax/PLA fibers within the mat, confirming the nominally (in-plane) random fiber distribution, which was also preserved in the fabricated PLA molded composite plaques (Figure 2c). The web-forming technique employed here was therefore successful in air-laying nonwoven webs with isotropic fiber orientation distribution.

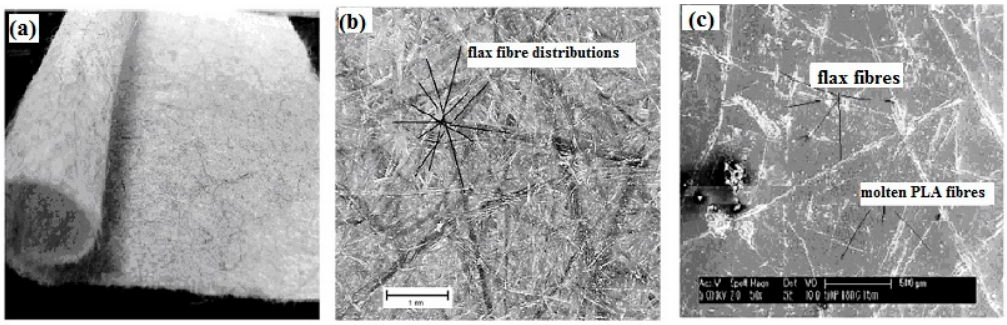

Figure 2. Image of produced flax/PLA nonwoven mat (**a**), flax fiber arrangement within the mat (**b**) and molded composite plaque (**c**).

Matrix dissolution tests on the consolidated NM flax/PLA and UD flax/PLA composites measured a flax fiber mass fraction (W_f) of 48.0% and 49.5%, respectively, similar to the measurements of the unconsolidated preforms. From Table 3 it was found that the calculated density of the nonwoven panel was found to be lower (1.1 g/cm^3) than the aligned panel (1.2 g/cm^3), due to the higher void content (18%) of the nonwoven panel. The latter is indicative of poor impregnation of the flax fibers by the PLA matrix during hot-press molding and suggests that matrix flow was adversely affected by the random orientation of flax fibers in the nonwoven mat composites, despite the use of a higher molding pressure (in comparison to the aligned panel). On the other hand, the calculated porosity content in UD flax/PLA composites was found to be significantly lower (4%). The results indicate that fiber architecture plays an important role on porosity level. The higher void content and greater

thickness of the NM flax/PLA composites also led to relatively lower fiber volume fraction (34.3%) compared to that of UD/PLA flax composites (38.6%).

Table 3. Physical and mechanical properties of unreinforced PLA and the composites.

Properties	Neat PLA	Random Flax/PLA	Aligned Flax/PLA
Flax fiber content (wt.%)	0.0	48.0	49.5
Composite density (g/cm^3)	1.24	1.1	1.2
Void content (%)	0.5	18.0	4.0
Tensile strength (MPa)	40.0 ± 3.0	83.0 ± 5.0	151.0 ± 7.0
Tensile modulus (GPa)	3.8 ± 1.0	9.3 ± 1.5	18.5 ± 2.0
Flexural strength (MPa)	82.0 ± 2.0	130.0 ± 5.0	215.0 ± 17.2
Flexural modulus (GPa)	4.0 ± 0.5	9.9 ± 1.0	18.8 ± 1.0
Specific tensile strength ($MPa^{1/2}$. cm^3/g)	5.3	7.7	10.3
Specific tensile modulus ($GPa^{1/3}$. cm^3/g)	1.2	1.8	2.2
Specific flexural strength ($MPa^{1/2}$. cm^3/g)	7.3	10.4	12.2
Specific flexural modulus ($GPa^{1/3}$. cm^3/g)	1.3	2.0	2.2

From Table 3, it was found that the tensile strength of neat PLA was measured to be 40 MPa; this was increased to 83 MPa and 151 MPa with random mat flax reinforcements and unidirectional flax reinforcements, respectively. The tensile modulus of aligned flax composites (18.5 GPa) was also found to be approximately double the random flax composites (9.3 GPa). Similar trends were found in flexural properties, where flexural strength and flexural modulus of UD flax/PLA composites was 60 and 70% higher respectively than NM flax/PLA composites.

Typical tensile stress-strain curves of neat PLA matrix, random flax/PLA composite and aligned flax/PLA composite are shown in Figure 3. In the figure, neat PLA shows a more linear behavior while the composites behave more nonlinearly as the strain increases. The linear phase corresponds to the linear deformation of the fiber and matrix while the nonlinear deformation of the composites has been explained as a three-phase mechanism by Panthapulakkal and Sain [37]. Firstly, the microcrack initiates at the fiber-end/matrix interface and propagates along the fiber lengths; secondly, the matrix undergoes plastic deformation; and finally the microcracks in the matrix open and propagate through the deformed matrix. Due to the pulling out of fibers from the matrix, catastrophic crack propagation also takes place through the matrix. The tensile properties of the biocomposite are higher than neat PLA after the incorporation of flax fiber as anticipated.

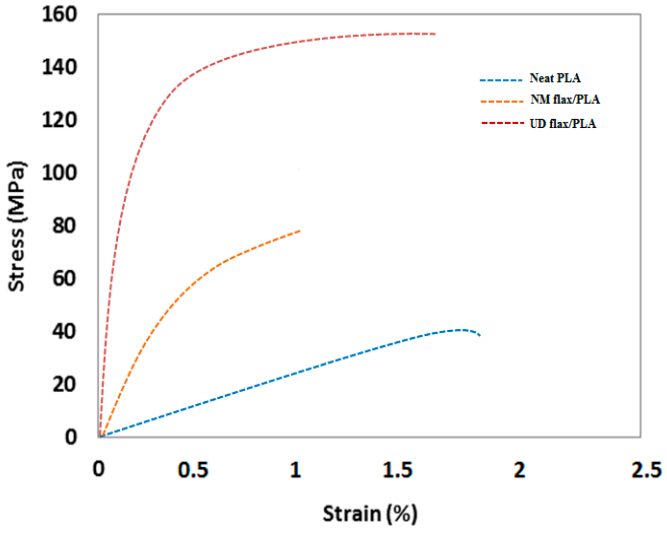

Figure 3. Tensile stress-strain curves of neat PLA and flax/PLA composites.

The significantly better mechanical properties of aligned fiber composites are mainly due to full fiber alignment in the loading direction. It would be expected that properties in the transverse direction of the aligned fiber composites would be comparably lower than those of the isotropic random mat composites. The void content also influences the quality (properties) of the composites. Voids have a negative impact on the mechanical properties of the composites since void can cause weaker bonding. Due to the presence of higher voids in the random fiber composites the mechanical properties were significantly deteriorated.

The fracture surfaces of random fiber composites (Figure 4a), examined through SEM, exhibited substantial fiber debonding and pull-out, which is indicative of poor fiber-matrix adhesion, possibly due to high porosities and dry zones within the composite. Figure 4b presents very little amount of fiber pull-out and lower porosity content specifies good fiber-matrix adhesion in the aligned fiber composites and those fiber properties are extensively transferred to the composite via matrix.

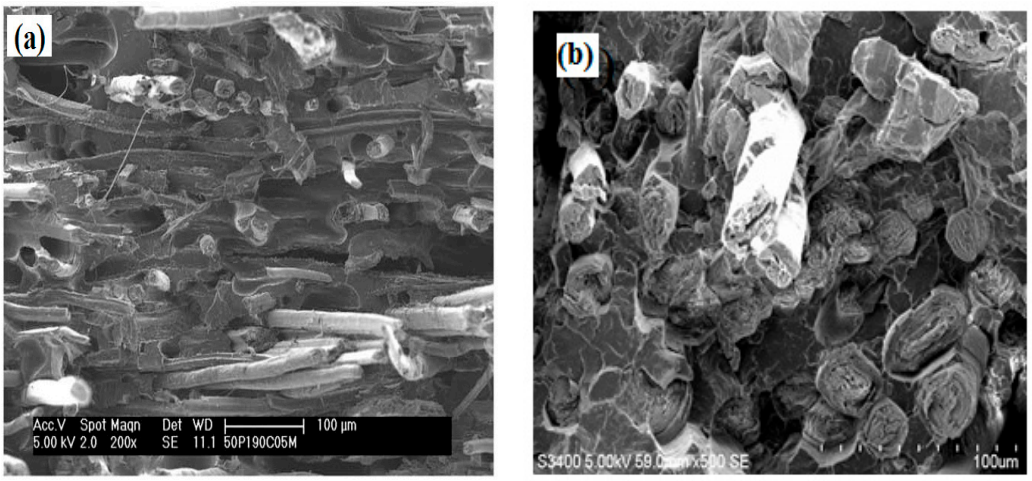

Figure 4. SEM images of tensile fracture surfaces of random fiber oriented (**a**) and unidirectional flax/PLA composites (**b**).

In Table 3, the calculated result of specific flexural strength and specific flexural modulus of both random and aligned panels were given. Both these parameters can be used as material performance indices for the selection of materials in stiffness or strength-critical, light-mass applications, such as an automotive load-floor panel in bending mode. The stiffness-density Ashby chart in Figure 5 compares the performance of the random and aligned flax/PLA composites with other engineering polymers and composites. All the materials that lie on the dashed guide line would give a panel with the same material index parameter, while a panel from materials to the left of the guide line would produce a stiffer panel of the same mass (or lighter panel of same stiffness). It was found that both random mat and aligned flax reinforced PLA thermoplastic panels performed better than wood products but performed worse than conventional glass and carbon fiber polymer composites. It was also revealed that the aligned panel has higher specific strength and stiffness values compared to random mat panel. The specific tensile strength and specific tensile modulus were found to be 10.3 ($MPa^{1/2}$. cm^3/g) and 2.2 ($GPa^{1/3}$. cm^3/g) respectively for UD flax/PLA composites. These values are very much compatible with woven E-glass/Epoxy composites [27]. Therefore, it might be a good choice to replace the woven E-glass/Epoxy composite with this UD flax/PLA panel, where stiffness is more important than strength. Moreover, flax fiber/PLA composite has an extra advantage over glass composite, as it is biodegradable.

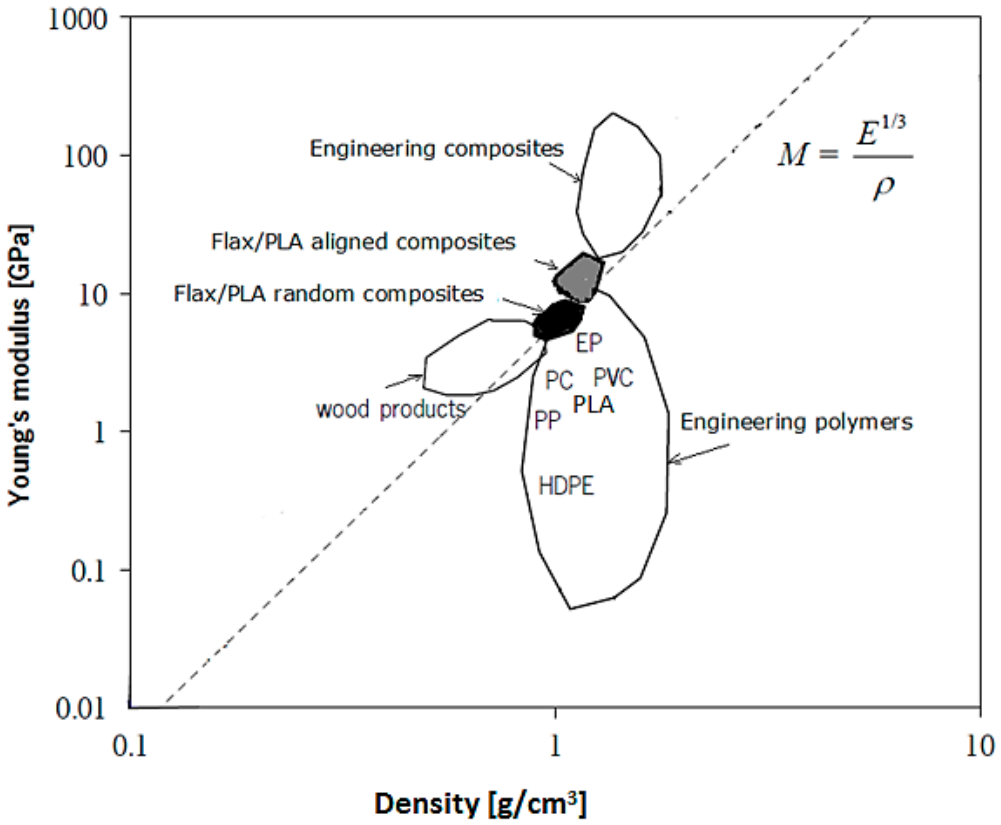

Figure 5. Materials performance chart comparing tensile modulus and density of random and aligned flax/PLA composites with common engineering polymers and composites. The dashed guide line enables materials selection for minimum mass, stiffness-limited design.

Figures 6 and 7 shows the DSC curves of the first and second heating cycle respectively of neat PLA and flax/PLA biocomposites. T_g and T_m were determined from the data of the first heating cycle, as T_g of composite samples was not visible in the second heating cycles, although the T_m differs slightly from the first heating cycle. This is probably due to the relatively slow cooling rate used which led to the crystallization of PLA. The obtained results are summarized in Table 4.

It was observed from Figures 6 and 7 that the glass transition temperature of neat PLA is higher than the values for biocomposites. The introduction of flax fiber decreases the temperature. The lower T_g value indicates the ductility of the composites reduced which may lead to lower impact strength. Non-satisfying impact resistance and low heat distortion temperature can restrict the application of flax/PLA composites in engineering fields [27]. It is also evident that the addition of flax fibers decreases the melting and onset melting temperature and the heat of fusion of the composites marginally because flax fiber acts as a diluent in the PLA matrix.

For UD flax composite, the value of T_g and T_m are higher than NM flax composite. This increase is likely a result of decreasing space available for molecular motion. It was also found that the crystallinity (%) of UD flax/PLA was much higher than NM flax/PLA composites.

In terms of biodegradation assessment of the composite panels, water absorbency performance, mass-loss and residual flexural properties of burial tested samples were investigated.

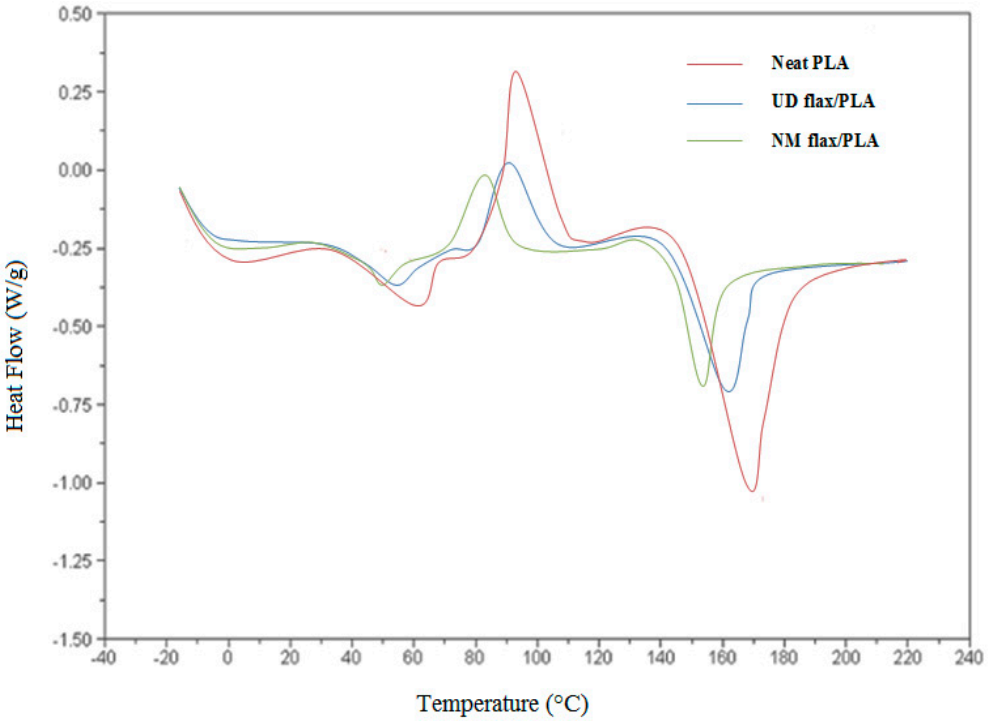

Figure 6. DSC curves of first heating cycle as a function of temperature of neat PLA and flax/PLA biocomposites.

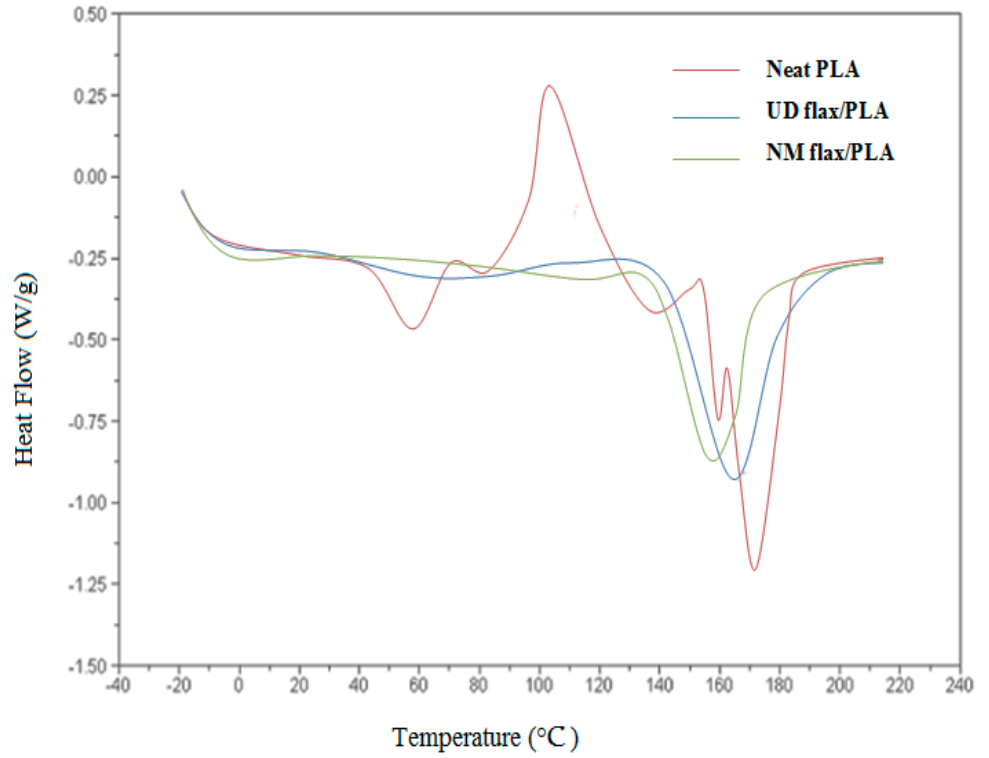

Figure 7. DSC curves of second heating cycle as a function of temperature of neat PLA and flax/PLA biocomposites.

Table 4. Thermal properties of neat PLA and flax/PLA biocomposites.

Sample	Glass Transition Temperature, T_g (°C)	Melting Temperature, T_m (°C)		Melting Enthalpy, ΔH_m (J/g)	Degree of Crystallinity, X_c (%)
		Onset Melting Temperature	Peak Melting Temperature		
Neat PLA	59	160	171	43	46
NM flax/PLA	50	145	155	32	34
UD flax/PLA	54	151	163	39	42

Water absorbency is expressed in terms of mass percentage gain of the composites. It is observed from Figure 8 that, after 60 days soaking period, the NM Flax/PLA composites absorbed water 40% of its mass, which is much higher than that of neat PLA and UD flax/PLA composites. The neat PLA and UD/flax composite absorbed 6 and 11% water respectively at the same time. It was also evident that incorporating flax fibers into the PLA matrix increased water absorption. This can be explained by the higher moisture absorption by the flax fibers. This was also reflected in the measurements of the degree of crystallinity; neat PLA had a crystallinity of 46%, reducing to 34 and 42% for the random and aligned fiber composites, respectively. Flax fibers have a greater amorphous fraction (in the range of 50–70% by dry mass than neat PLA [38] and it is agreed that amorphous regions are more susceptible to moisture absorption and biodegradation [39]. Furthermore, flax fibers composed of almost 70% cellulose and 20% hemicellulose polysaccharides which have a large number of polar hydrophilic –OH groups [40]. In addition, the higher void content of the fiber reinforced composites, in particular, the random mat composites may have a role in accelerating water absorption. In this way, water/moisture initiates the biodegradation process of flax/PLA laminate [30].

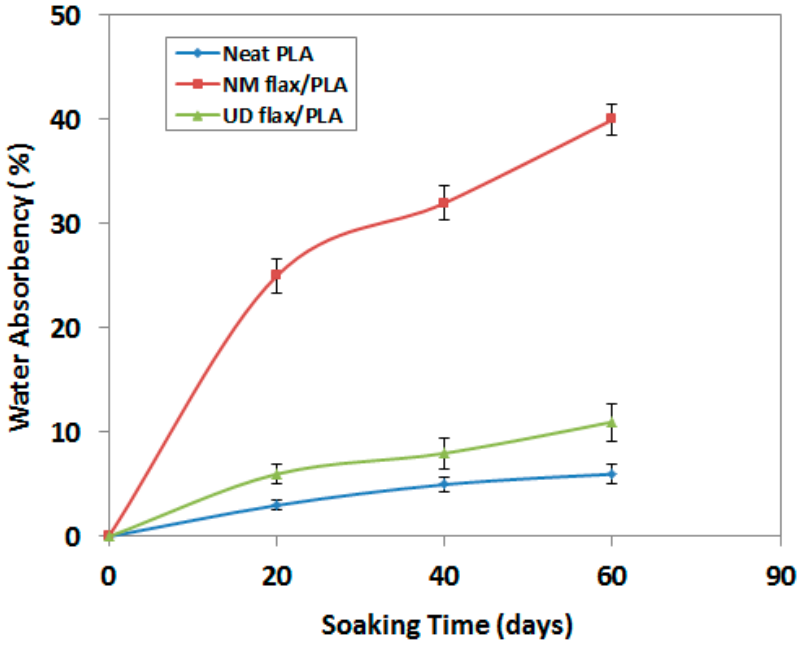

Figure 8. Water absorbency performance of unreinforced and flax reinforced PLA.

Figures 9 and 10 displayed the mass loss (%) of the flax fibers, neat PLA and their composites as a function of burial time. Rapid mass loss (biodegradation) was occurred for flax fibers. From Figure 9 it was found that after 120 days flax fibers lost 90% mass and neat PLA showed minimal (10%) mass loss. Rapid biodegradation action was observed for random mat composites; after 120 days of burial time 27% mass loss was reported while aligned panels exhibited much lower mass loss (19%) over the same period (Figure 10), which was due to lower moisture/water swelling performance of this panel. In Figure 11, SEM images of neat PLA and NM flax/PLA show the evidence of biodegradation,

where biodegradation of the matrix started after 60 days. However, SEM images demonstrate that the biodegradation of flax and its composites can start from 30 days in a suitable natural environment (Figure 11f).

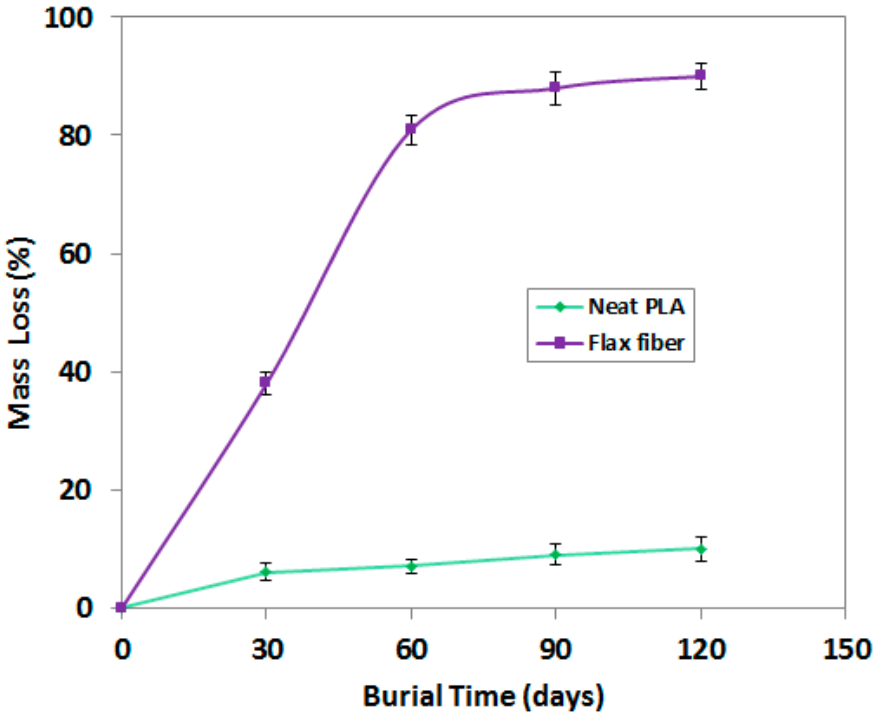

Figure 9. Effect of biodegradations on PLA and flax fibers.

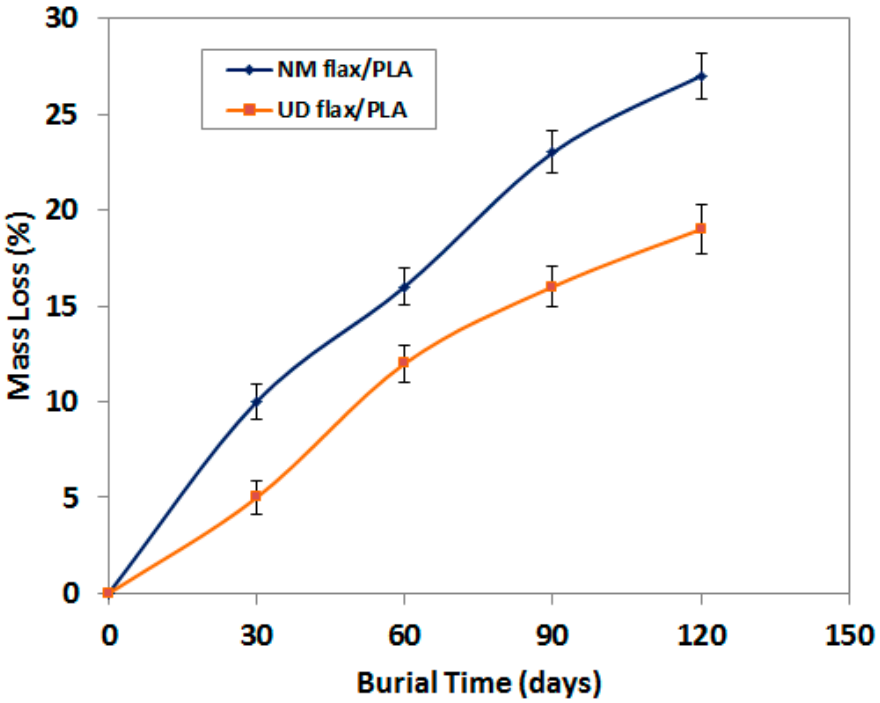

Figure 10. Effect of biodegradations on Flax/PLA composites.

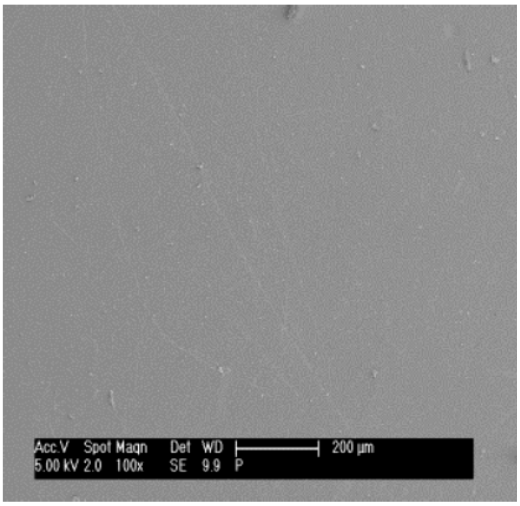

(**a**) PLA 0 days

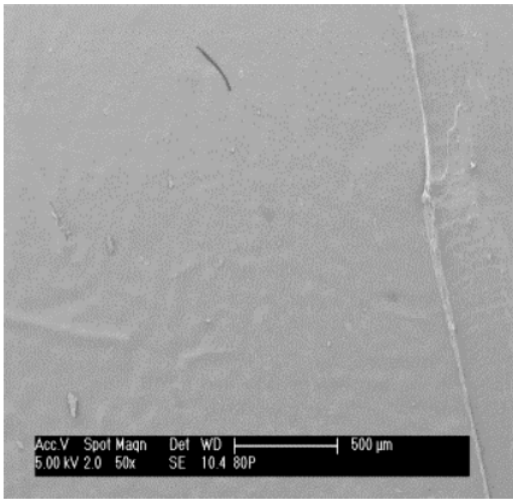

(**b**) PLA 30 days

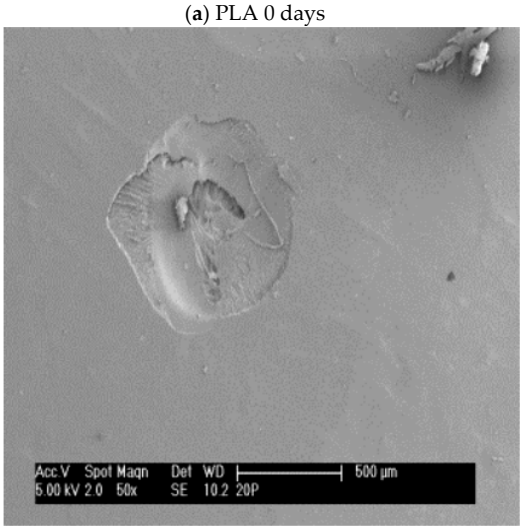

(**c**) PLA 60 days

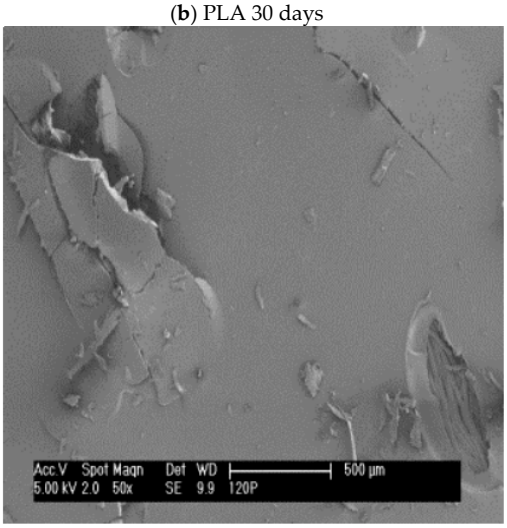

(**d**) PLA 120 days

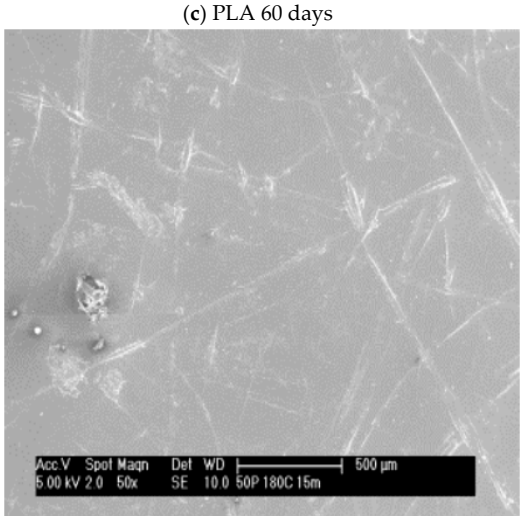

(**e**) NM flax/PLA 0 days

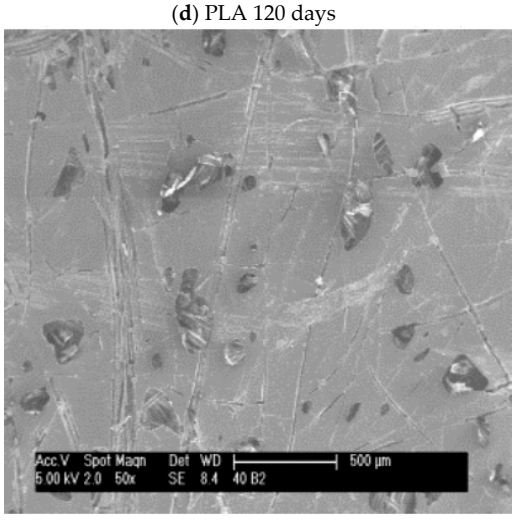

(**f**) NM flax/PLA 30 days

Figure 11. *Cont*.

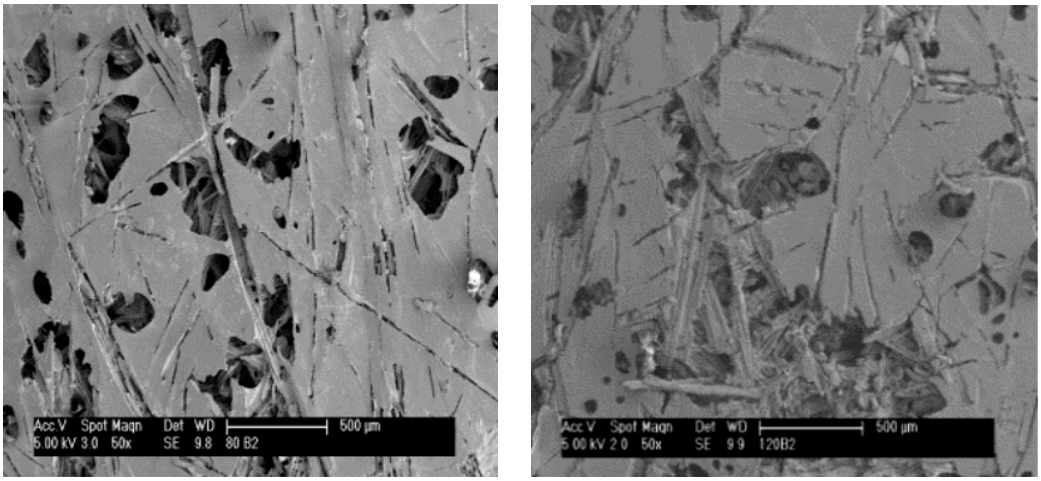

(**g**) NM flax/PLA 60 days (**h**) NM flax/PLA 120 days

Figure 11. SEM images of biodegradation effect on neat PLA (**a**–**d**) and NM flax/PLA composites (**e**–**h**).

This biodegradation also triggers a reduction in the mechanical performances of the panels. Figures 12 and 13 indicates that the flexural properties (strength and modulus) of NM flax/PLA composites dropped (by 80%) significantly after 120 days burial test, whereas at that time the flexural strength of neat PLA and UD flax/PLA panels was reduced by 37 and 57%, respectively. The damage of modulus was 20 and 50% for these samples, respectively after 120 days burial time. In all cases, the major loss in properties was within 30 days of burial. The degradation of the properties (particularly stiffness) of random mat panels was substantially greater in comparison to aligned flax panels due to the former's higher water absorbency and subsequent rapid biodegradation, particularly of the flax fiber reinforcement constituent. Due to the presence of more voids in NM flax/PLA panel, it was degraded more after 120 days of burial time which was also observed in Figure 12.

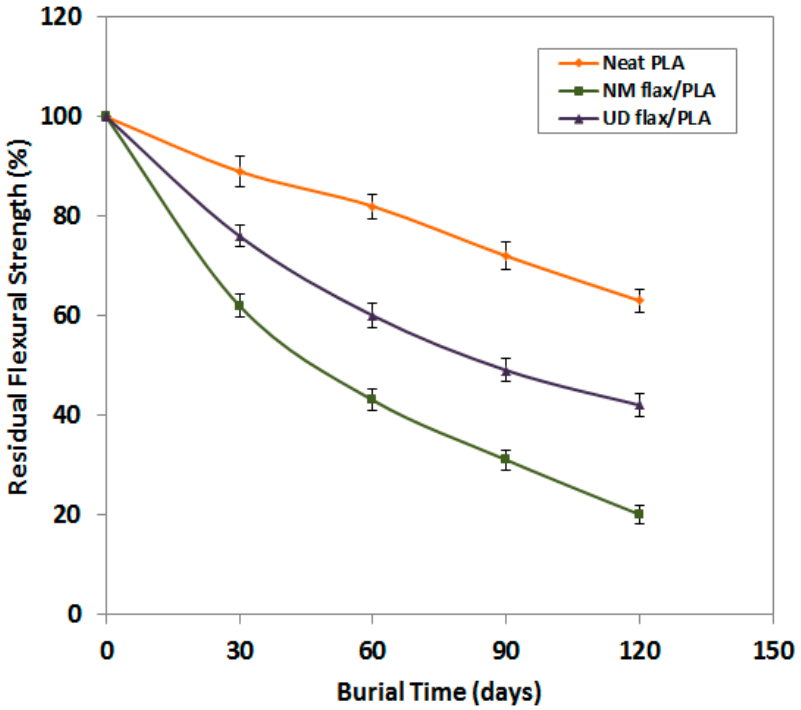

Figure 12. Comparative residual flexural strength of biodegraded composites.

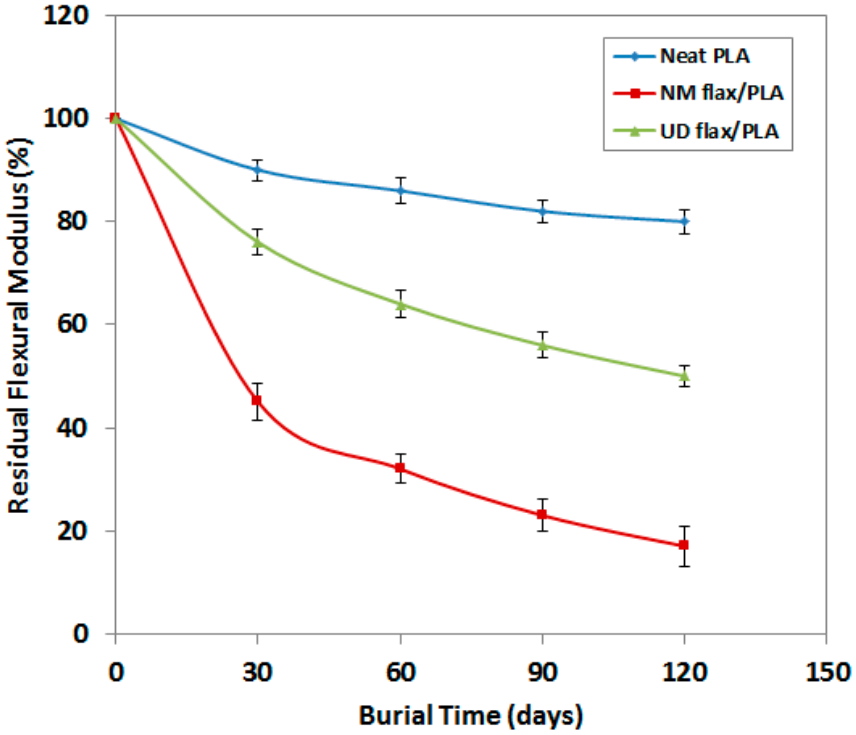

Figure 13. Comparative residual flexural modulus of biodegraded composites.

During soil burial tests, flax fiber is attacked by macro-organisms and micro-organisms. Biodegradation is chiefly introduced by the action of various micro-organisms and the action of micro–organisms are closely associated with the presence of water in soil [41,42]. Macro–organisms may degrade the biocomposites. Flax fiber is composed of cellulose, lignin and pectin which are entirely biodegradable and therefore, the flax fiber is completely biodegradable. On the other hand, the matrix PLA used in this work is also biodegradable. Thus, both the component materials in the manufactured composite are being broken down by micro and macro organisms and enhance the biodegradation. In the case of neat PLA, the biodegradation performance may be attributed to the preferential hydrolysis (breaking up of the polymer into smaller units) [43,44]. The hydrolytic reaction may occur when -$CHCH_3COO$–groups on PLA molecules react with H_2O and produce low molecular mass biocomposites with increased carboxylic groups in the polymer chain (Equation (12)) [43].

$$\text{-}CHCH_3COO- + H_2O \rightarrow \text{-}CHCH_3OH + HOOC\text{-} \quad (12)$$

However, for biocomposites, the biodegradation effect is combined with the fiber-matrix interface degradation. Hydrolytic matrix degradation and fiber debonding may lead to a lower adhesion at the interface and subsequently, to poorer mechanical properties. The influences of the biological environment on the structural change of composites are supported by the SEM image of PLA and NM flax/PLA composites (Figure 11). Nevertheless, the biodegradation effects were delayed for the aligned panel as it was structurally compacted (fibers were well-impregnated by molten matrix) with few voids, therefore, this panel was found more resistant to biodegradation action. If SEM could be done on UD flax/PLA panels then it would be more helpful to understand.

4. Conclusions

In this work, two types of composites, one made of NM flax/PLA and the other one made of UD flax/PLA, were manufactured and their performance was investigated. The results revealed that both types of composites are much stronger than neat PLA as expected. More importantly, the UD flax/PLA showed significantly improved mechanical properties compared to NM flax/PLA. Although

both composites consist of same flax fibers (by mass), due to the fiber orientation to the direction of the applied stress, aligned fiber composite provided superior performance under both tensile and bending mode. The tensile and flexural strength of UD flax/PLA composite was increased 82 and 65% respectively and the tensile and flexural modulus was improved 99 and 90% respectively compared to NM flax/PLA composite. The rate of biodegradation of UD flax/PLA structure was also found considerably lower than NM flax/PLA composites due to lower swelling performance. The flexural property of neat PLA, NM flax/PLA and UD flax/PLA are significantly decreased after soil burial. During soil burial test, the UD flax/PLA and NM flax/PLA lost 19 and 27% mass respectively after 120 days observation, the residual flexural strength reduced by 57 and 80% respectively and flexural modulus decreased by 50 and 80% respectively for UD flax/PLA and NM flax/PLA at the same time. The results were confirmed by SEM observations which showed the presence of many large holes and more cracks in the degraded surface of the biocomposites. Significant amount of cavities were found on the surface of the composites which accelerates the biodegradation. Additionally, hydrolysis process may be involved in the degradation of PLA, reducing the properties of the matrix and degrading the interfacial bonding between PLA and flax by molar mass degradation. Specific rigidity values of the composites in bending mode showed that both flax/PLA materials outperform the woven glass fiber reinforced epoxy composite and can replace glass fibers, particularly where stiffness is more important than strength. In terms of environmental impact, biodegradability is a clear advantage of flax/PLA composite than glass fiber reinforced composites as flax/PLA composite is decomposable. Altogether, based on analysis, direct contact with water medium is the most deteriorating environment for biocomposites and therefore underwater applications of these materials are strongly discouraged. However, the results found in the study may be acceptable for the users who are planning to use biodegradable composites in standard atmosphere and for short-term applications in the humid or wet environment.

Author Contributions: M.H.A. and S.A. designed the research work; D.U.S. and A.N.M.M.R. performed all the experiments; M.H.A. and A.N.M.M.R. analyzed the data and prepared the manuscript; all the authors reviewed and edited the final paper.

Funding: The research received no external funding.

Acknowledgments: The authors would like to thank Tilsatec Advanced Textile Materials (UK) and Bangladesh University of Textiles, Bangladesh for supporting this work.

Conflicts of Interest: The authors declare no conflict of interest.

References

1. Mohanty, A.K.; Misra, M.; Drzal, L.T. *Natural Fibers, Biopolymers and Biocomposites*; CRC Press: Boca Raton, FL, USA, 2005.
2. Wallenberger, F.T.; Weston, N. *Natural Fibers, Plastics and Composites*; Springer Science & Business Media: New York, NY, USA, 2003.
3. Awal, A.; Rana, M.; Sain, M. Thermorheological and mechanical properties of cellulose reinforced PLA bio-composites. *Mech. Mater.* **2015**, *80*, 87–95. [CrossRef]
4. Garlotta, D. A literature review of poly (lactic acid). *J. Polym. Environ.* **2001**, *9*, 63–84. [CrossRef]
5. Markarian, J. Biopolymers present new market opportunities for additives in packaging. *Plast. Addit. Compd.* **2008**, *10*, 22–25. [CrossRef]
6. Vroman, I.; Tighzert, L. Biodegradable polymers. *Materials* **2009**, *2*, 307–344. [CrossRef]
7. Yusoff, R.B.; Takagi, H.; Nakagaito, A.N. Tensile and flexural properties of polylactic acid-based hybrid green composites reinforced by kenaf, bamboo and coir fibers. *Ind. Crops Prod.* **2016**, *94*, 562–573. [CrossRef]
8. Mohanty, A.K.; Misra, M.; Drzal, L. Sustainable bio-composites from renewable resources: Opportunities and challenges in the green materials world. *J. Polym. Environ.* **2002**, *10*, 19–26. [CrossRef]
9. Burgueno, R.; Quagliata, M.J.; Mohanty, A.K.; Mehta, G.; Drzal, L.T.; Misra, M. Load-bearing natural fiber composite cellular beams and panels. *Compos. Part A Appl. Sci. Manuf.* **2004**, *35*, 645–656. [CrossRef]

10. Sahoo, S.; Misra, M.; Mohanty, A.K. Enhanced properties of lignin-based biodegradable polymer composites using injection molding process. *Compos. Part A Appl. Sci. Manuf.* **2011**, *42*, 1710–1718. [CrossRef]
11. Cabral, H.; Cisneros, M.; Kenny, J.; Vazquez, A.; Bernal, C. Structure–properties relationship of short jute fiber-reinforced polypropylene composites. *J. Compos. Mater.* **2005**, *39*, 51–65. [CrossRef]
12. Jayaraman, K. Manufacturing sisal–polypropylene composites with minimum fibre degradation. *Comput. Sci. Technol.* **2003**, *63*, 367–374. [CrossRef]
13. Madsen, B.; Hoffmeyer, P.; Thomsen, A.B.; Lilholt, H. Hemp yarn reinforced composites—I. Yarn characteristics. *Compos. Part A Appl. Sci. Manuf.* **2007**, *38*, 2194–2203. [CrossRef]
14. Feng, D.; Caulfield, D.; Sanadi, A. Effect of compatibilizer on the structure-property relationships of kenaf-fiber/polypropylene composites. *Polym. Compos.* **2001**, *22*, 506–517. [CrossRef]
15. Baiardo, M.; Zini, E.; Scandola, M. Flax fibre–polyester composites. *Compos. Part A Appl. Sci. Manuf.* **2004**, *35*, 703–710. [CrossRef]
16. Rubio-López, A.; Artero-Guerrero, J.; Pernas-Sánchez, J.; Santiuste, C. Compression after impact of flax/PLA biodegradable composites. *Polym. Test.* **2017**, *59*, 127–135. [CrossRef]
17. Yan, L.; Chouw, N.; Jayaraman, K. Flax fibre and its composites–A review. *Compos. Part B Eng.* **2014**, *56*, 296–317. [CrossRef]
18. Lucintel, B. *Opportunities in Natural Fiber Composites*; Texas Lucintel: Dallas, TX, USA, 2011.
19. Saravana Bavan, D.; Mohan Kumar, G. Potential use of natural fiber composite materials in India. *J. Reinf. Plast. Compos.* **2010**, *29*, 3600–3613. [CrossRef]
20. Murariu, M.; Dubois, P. PLA composites: From production to properties. *Adv. Drug Del. Rev.* **2016**, *107*, 17–46. [CrossRef]
21. La Mantia, F.; Morreale, M. Green composites: A brief review. *Compos. Part A Appl. Sci. Manuf.* **2011**, *42*, 579–588. [CrossRef]
22. Koronis, G.; Silva, A.; Fontul, M. Green composites: A review of adequate materials for automotive applications. *Compos. Part B Eng.* **2013**, *44*, 120–127. [CrossRef]
23. Foruzanmehr, M.; Vuillaume, P.Y.; Elkoun, S.; Robert, M. Physical and mechanical properties of PLA composites reinforced by TiO_2 grafted flax fibers. *Mater. Des.* **2016**, *106*, 295–304. [CrossRef]
24. Lim, L.-T.; Auras, R.; Rubino, M. Processing technologies for poly (lactic acid). *Prog. Polym. Sci.* **2008**, *33*, 820–852. [CrossRef]
25. Ma, H.; Joo, C.W. Structure and mechanical properties of jute—Polylactic acid biodegradable composites. *J. Compos. Mater.* **2011**, *45*, 1451–1460.
26. Shanks, R.; Hodzic, A.; Ridderhof, D. Composites of poly (lactic acid) with flax fibers modified by interstitial polymerization. *J. Appl. Polym. Sci.* **2006**, *101*, 3620–3629. [CrossRef]
27. Couture, A.; Lebrun, G.; Laperrière, L. Mechanical properties of polylactic acid (PLA) composites reinforced with unidirectional flax and flax-paper layers. *Compos. Struct.* **2016**, *154*, 286–295. [CrossRef]
28. Alimuzzaman, S.; Gong, R.H.; Akonda, M. *Impact Property of PLA/flax Nonwoven Biocomposite*; Conference Papers in Materials Science; Hindawi: New York, NY, USA, 2013.
29. Lee, S.H.; Kang, T.J. Mechanical and impact properties of needle punched nonwoven composites. *J. Compos. Mater.* **2000**, *34*, 816–840. [CrossRef]
30. Alimuzzaman, S.; Gong, R.H.; Akonda, M. Nonwoven polylactic acid and flax biocomposites. *Polym. Compos.* **2013**, *34*, 1611–1619. [CrossRef]
31. Hearle, J.; Stevenson, P. Nonwoven fabric studies: Part III: The anisotropy of nonwoven fabrics. *Text. Res. J.* **1963**, *33*, 877–888. [CrossRef]
32. Krenchel, H. *Fibre Reinforcement; Theoretical and Practical Investigations of the Elasticity and Strength of Fibre-Reinforced Materials*; Akademisk Forlag: Copenhagen, Denmark, 1964.
33. Bledzki, A.K.; Jaszkiewicz, A.; Scherzer, D. Mechanical properties of PLA composites with man-made cellulose and abaca fibres. *Compos. Part A Appl. Sci. Manuf.* **2009**, *40*, 404–412. [CrossRef]
34. Kim, H.-S.; Kim, H.-J.; Lee, J.-W.; Choi, I.-G. Biodegradability of bio-flour filled biodegradable poly (butylene succinate) bio-composites in natural and compost soil. *Polym. Dégrad. Stab.* **2006**, *91*, 1117–1127. [CrossRef]
35. Kim, H.S.; Yang, H.S.; Kim, H.J. Biodegradability and mechanical properties of agro-flour–filled polybutylene succinate biocomposites. *J. Appl. Polym. Sci.* **2005**, *97*, 1513–1521. [CrossRef]
36. Alimuzzaman, S.; Gong, R.H.; Akonda, M. Biodegradability of nonwoven flax fiber reinforced polylactic acid biocomposites. *Polym. Compos.* **2014**, *35*, 2094–2102. [CrossRef]

37. Panthapulakkal, S.; Sain, M. Injection-molded short hemp fiber/glass fiber-reinforced polypropylene hybrid composites—Mechanical, water absorption and thermal properties. *J. Appl. Polym. Sci.* **2007**, *103*, 2432–2441. [CrossRef]
38. Satyanarayana, K.G.; Arizaga, G.G.; Wypych, F. Biodegradable composites based on lignocellulosic fibers—An overview. *Prog. Polym. Sci.* **2009**, *34*, 982–1021. [CrossRef]
39. Plackett, D.; Andersen, T.L.; Pedersen, W.B.; Nielsen, L. Biodegradable composites based on L-polylactide and jute fibres. *Compos. Sci. Technol.* **2003**, *63*, 1287–1296. [CrossRef]
40. John, M.J.; Anandjiwala, R.D. Recent developments in chemical modification and characterization of natural fiber-reinforced composites. *Polym. Compos.* **2008**, *29*, 187–207. [CrossRef]
41. Rudeekit, Y.; Numnoi, J.; Tajan, M.; Chaiwutthinan, P.; Leejarkpai, T. Determining biodegradability of polylactic acid under different environments. *J. Met. Mater. Miner.* **2008**, *18*, 83–87.
42. Kumar, R.; Yakubu, M.; Anandjiwala, R. Biodegradation of flax fiber reinforced poly lactic acid. *Express Polym. Lett.* **2010**, *4*, 423–430. [CrossRef]
43. Mohammad Khanlou, H.; Hall, W.; Woodfield, P.; Summerscales, J.; Francucci, G. The mechanical properties of flax fibre reinforced poly (lactic acid) bio-composites exposed to wet, freezing and humid environments. *J. Compos. Mater.* **2018**, *52*, 835–850. [CrossRef]
44. Bayerl, T.; Geith, M.; Somashekar, A.A.; Bhattacharyya, D. Influence of fibre architecture on the biodegradability of FLAX/PLA composites. *Int. Biodeterior. Biodégrad.* **2014**, *96*, 18–25. [CrossRef]